ISBN: 978-3-95450-210-3 doi:10.18429/JACoW-FEL2019-TUP092

XFEL THIRD HARMONIC STATISTICS MEASUREMENT AT LCLS

A. Halavanau, E. Hemsing, A. Lutman, C. Emma, G. Marcus, C. Pellegrini,
SLAC National Accelerator Laboratory, Stanford University, Menlo Park, USA

Abstract

We investigate the statistical properties of the 6 keV third harmonic XFEL radiation at 2 keV fundamental photon energy at LCLS. We performed third harmonic self-seeding in the hard X-ray self-seeding chicane and characterized the attained non-linear third harmonic spectrum. We compare theoretical predictions with experimental results.

INTRODUCTION

Third harmonic XFEL generation is often considered to be very useful for tripling the photon frequency in planar undulators. The odd harmonic wavelength on axis is given by

$$\lambda = \frac{\lambda_u}{2h\gamma^2}(1 + K^2/2). \tag{1}$$

where λ is the fundamental FEL radiation wavelength, λ_u is the undulator period with magnetic parameter K, $h = 3, 5, 7$ is the odd harmonic number. Initially, harmonics are evolving independently from the fundamental in the linear regime [1,2]. Very quickly, the linear regime is altered by the nonlinear bunching at the fundamental frequency, entering the nonlinear harmonic generation (NHG) regime [1–4]. Thus, most of the XFEL third harmonic power is generated in NHG regime, and is estimated to be a few percent level of the fundamental XFEL power [5].

It was shown, however, that harmonic power can be drastically increased by disrupting the fundamental, but letting third harmonic bunching continue to develop linearly. It can be done in numerous ways, e.g. introducing phase shifters to disrupt the fundamental, and/or by using frequency filters [2,3]. This process, known as "harmonic lasing", allows accessing high photon energies at much higher power level at existing XFEL facilities. It has been previously considered for LCLS-II operations in detail in [6]. Recently, harmonic lasing has been performed at DESY [3] and at Pohang Accelerator Laboratory [7] in EUV regime.

EXPERIMENTAL SETUP

In this proceeding, we study the possibility of using the LCLS hard X-ray self-seeding (HXRSS) chicane Diamond crystal as a frequency filter in an HXR harmonic lasing setup. The first experimental results were reported in [8]. Since the original LCLS HXR beamline did not have variable gap and phase-shifters, experimental demonstration of the harmonic lasing was challenging and it will be done when the new LCLS-II HXR undulator is available. Here we focus on analyzing recorded data for the NHG and third harmonic self-seeding processes.

Our experimental setup, presented in Fig. 1, generated 2 keV photons at fundamental in U1-U15 undulator section, and thereby produced 6 keV photons at the third harmonic. The LCLS pulse intensity was reduced by retracting first 3 undulators, to ensure a safe level of X-ray pulse energy absorbed by the diamond crystal. The generated non-linear third harmonic field was overlapped with the electron beam downstream of the HXRSS chicane, where the bunching at fundamental was removed. The Diamond crystal, while strongly absorbing the fundamental photon energy, propagated 6 keV photons with about 60 % attenuation. The LCLS HXR beamline experimental parameters are grouped in Table 1.

Table 1: LCLS HXR Beamline Parameters During the Measurements

Parameter	Units	Value
Pulse duration	fs	80
Pulse energy (xtal)	μJ	80
Fundamental	keV	2
Third harmonic	keV	6
Gain length	m	4.1
Beam current	kA	1800
Energy spread	MeV	2.0
Emittance (proj.)	μm	0.8

We registered the fundamental pulse energy with the gas intensity monitor and third harmonic spectra with a spectrometer. The data was then accumulated to provide spectral sums for the statistical analysis.

STATISTICAL PROPERTIES OF THE THIRD HARMONIC RADIATION

To derive the statistical properties of XFEL radiation at the fundamental frequency, we consider a chaotic ensemble of fully polarized sources [9]. It can be shown that a single mode probability density obeys negative exponential law:

$$p_1(I) = \frac{1}{\langle I \rangle} \exp\left(-\frac{I}{\langle I \rangle}\right). \tag{2}$$

Here I is the instantaneous single mode radiation intensity and $\langle I \rangle$ is its time average. Iteratively integrating using a convolution rule $p_2(W) = \int_0^W p_1(W-x)p_1(x)dx$, one

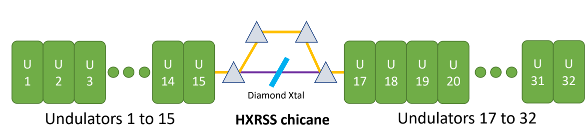

Figure 1: Experimental layout of XFEL third harmonic studies at LCLS.

ISBN: 978-3-95450-210-3 doi:10.18429/JACoW-FEL2019-TUP092

quickly arrives to a well-known formula often referred to as "Gamma" statistics

$$p_M(W) = \frac{M^M}{\Gamma(M)} \left(\frac{W}{\langle W\rangle}\right)^{M-1} \frac{1}{\langle W\rangle} \exp\left(-M\frac{W}{\langle W\rangle}\right), \quad (3)$$

where M has the physical meaning of number of modes in XFEL pulse. In the linear regime, higher harmonics are expected to follow the same probability law, with a different number of modes M [4].

In the nonlinear regime, for h-th odd harmonic radiation, one should take into account the h-th power scaling, therefore we transform $p_1(W) \to p_1^{(h)}(z)$ with $z = W^h$ [10]. Then the single mode probability density is given by

$$p_1^{(h)}(z) = \frac{1}{h\langle W\rangle} z^{(1-h)/h} \exp\left(-\frac{z^{1/h}}{\langle W\rangle}\right), \quad (4)$$

with $\int_0^\infty p_1^{(h)}(z)dz = 1$. Convolving with itself, we arrive to:

$$p_2^{(h)}(z) = \frac{1}{h^2\langle W\rangle^2} \int_0^z \left[z'(z-z')\right]^{(1-h)/h} \times \\ \times \exp\left(-\frac{z'^{1/h} + (z-z')^{1/h}}{\langle W\rangle}\right) dz' \quad (5)$$

Due to the difference in prefactor and in the exponential in Eq. (4), the integral in Eq. (5) becomes fundamentally different. Notice that any positive odd number h in $(1-h)/h$ yields a negative fraction, therefore the integrand in Eq. (5) has branching points at $0, z$. Integrating Eq. (5) for $h = 3$ and two and more modes in closed form becomes cumbersome and does not match with the "Gamma" law given by Eq. (3). Instead, S-fold mode convolutions can be integrated numerically to an arbitrary precision, ensuring the condition $\int_0^\infty p_S^{(3)}(z)dz = 1$ for any given number of third harmonic modes S.

COMPARISON WITH EXPERIMENTAL SPECTRA

To perform further inverstigation of the derived statistics, we analyze recorded spectra (see Fig. 2) and its statistics. Figure 3 displays numerically evaluated nonlinear third harmonic statistics for a different number of third harmonic modes S. For asymptotics analysis we plotted "Gamma" statistics that approximately matches the $p_S^{(3)}(z)$ alongside. Very interestingly, $p_S^{(3)}(z)$ asymptotically follows "Gamma" statistics with the relation for the number of modes $S/M_{fit} \approx 34$. We also provide a comparison of semi-analytically calculated probability density function with the measured experimental spectral sums in Fig. 3. Figure 3 also displays the fitted M in $p_S^{(3)}(z)$. Notice that initially S is large due to all modes of the nonlinear third harmonic passed through the filtering crystal. It is then slightly reduced between U17 and U22, and then increases downstream of U22. Overall, the derived statistics corroborates with the measurements to a very good extent.

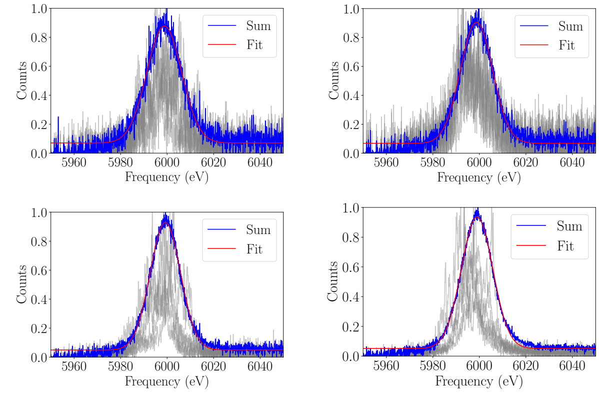

Figure 2: Shot-to-shot (gray) and cumulative spectra (blue) of the third harmonic at (left to right, top to bottom) U18, U20, U22 and U26 location.

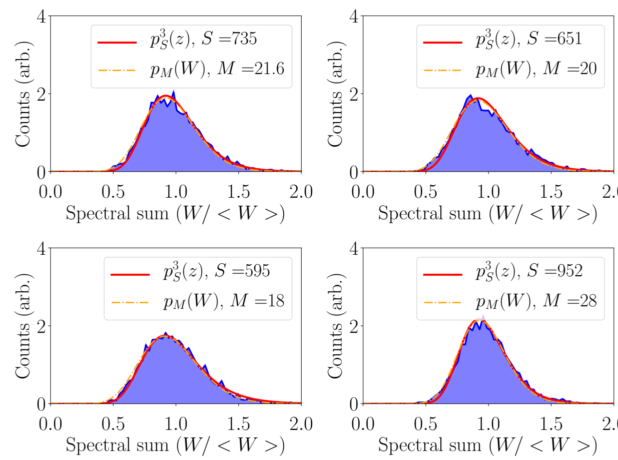

Figure 3: Histograms of spectral sums of the third harmonic radiation at (left to right, top to bottom) U18, U20, U22 and U26 location.

COMPARISON WITH STATISTICS OF THE FUNDAMENTAL

An interesting comparison can be drawn from the fundamental statistics of the XFEL pulse, recorded by the gas intensity monitor. We will use RMS fluctuations given by

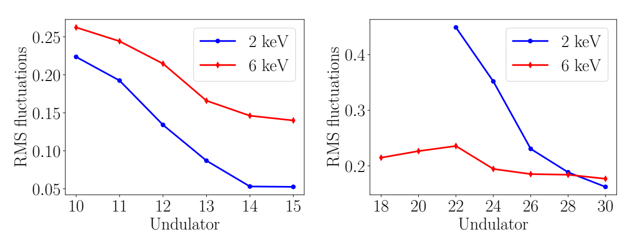

Figure 4: RMS fluctuations of the fundamental (2 keV) and third harmonic (6 keV) radiation intensity as a function of LCLS HXR undulator number.

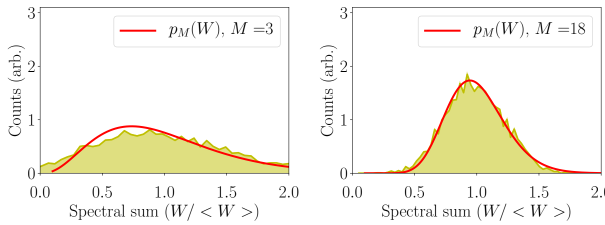

Figure 5: Statistics of the fundamental 2 keV radiation intensity at U22 (left) and U26 (right) location.

the following relation

$$\sqrt{\frac{\sigma_W^2}{W^2}} = \frac{1}{\sqrt{M}}, \tag{6}$$

where W is the intensity, σ_W^2 is the intensity variance, and M is approximately the number of Poisson modes given by (2). Ref. [4] gives an estimate of non-linear third harmonic RMS fluctuations to be 4 times more noisy (see Eq. (B10) in [4]). This estimate is provided for the case of the exponential SASE regime of the fundamental. In our experiment, we first drove 2 keV fundamental photon energy close to saturation, in order to generate large number photons at 6 keV [8].

Comparison of RMS intensity fluctuations is presented in Fig. 4. We observe the discrepancy of about factor of 2 with theoretically predicted value, possibly attributed to the noise in gas intensity monitor that was used to record the fundamental. Additionally being close to saturation in fundamental photon energy alters the assumptions of Ref. [4]. The direct measurement of the third harmonic statistics in various regimes require additional preparation of the detector hardware and will be performed separately.

We provide a comparison between fundamental and third harmonic RMS fluctuations in Fig. 4. As expected, the non-linear third harmonic has more fluctuations than fundamental; see Fig. 4, left. When going to the case of self-seeding, fundamental starts to develop around U22, and the “Gamma” statistics emerge as seen in Fig. 5. Thus, XFEL radiation field enters an interesting regime, where the statistical RMS fluctuations of both fundamental and third harmonic are equal.

SUMMARY AND CONCLUSIONS

In summary, we have analyzed recorded spectra for XFEL fundamental 2 keV and third harmonic 6 keV photon energy. We derived semi-analytical model for the third harmonic statistics and observed an agreement between the data and our model. We demonstrate that non-linear third harmonic statistics in case of large number of modes asymptotically follows the “Gamma” and eventually Gaussian statistics. Existing LCLS-II HXRSS chicane infrastructure can be used for future third harmonic self-seeding and harmonic lasing experiments. We present here a special case when both fundamental and third harmonic attain the same level of statistical fluctuations in the process of third harmonic self-seeding.

We note that combining our setup with the new variable gap LCLS-II HXR undulator and phase-shifters will significantly enhance harmonic lasing process at HXR photon energy. The results of these studies will be reported elsewhere.

ACKNOWLEDGEMENTS

This work was supported by the U.S. Department of Energy Contract No. DE-AC02-76SF00515 and award no. 2017-SLAC-100382. Authors would like to thank Z. Huang for the valuable suggestions throughout the research. A.H. is grateful to E. Schneidmiller for many discussions on this topic during IPAC19 conference.

REFERENCES

[1] R. Bonifacio, L. De Salvo Souza, P. Pierini, and E. T. Scharlemann. *NIM:A*, 296:787–790, (1990). doi:10.1016/0168-9002(90)91307-W

[2] B. W. J. McNeil, G. R. M. Robb, M. W. Poole, and N. R. Thompson. *Phys. Rev. Lett.*, 96:084801, (2006). doi:10.1103/PhysRevLett.96.084801

[3] E. A. Schneidmiller and M. V. Yurkov. *Phys. Rev. ST Accel. Beams*, 15:080702, (2012). dpo:10.1103/PhysRevSTAB.15.080702 [Erratum: Phys. Rev. ST Accel. Beams, 15:119901, (2012)]. doi:10.1103/PhysRevSTAB.15.119901

[4] Z. Huang and K.-J. Kim. *Phys. Rev. E*, 62:7295–7308, (2000). doi:10.1103/PhysRevE.62.7295

[5] D. Ratner, *et al*, *Phys. Rev. ST Accel. Beams*, 14:060701, 2011. doi:10.1103/PhysRevSTAB.14.060701

[6] G. Marcus, Y. Ding, Z. Huang, T. Raubenheimer, G. Penn, “Harmonic lasing options for LCLS-II”, *Report No. SLAC-PUB-16081*, (2014).

[7] I. Nam, C.-K. Min, C. Kim, H. Yang, G. Kim, H. Heo, S. Kwon, S. H. Park, and H.-S. Kang. *Applied Physics Letters*, 112(21):213506, (2018). doi:10.1063/1.5030443

[8] C. Emma, *et al*, In *Proc. of, IPAC2019 Melbourne, Australia, May 19-24, 2019*, page TUPRB091, 2019. doi:10.18429/JACoW-IPAC2019-TUPRB091

[9] J.W. Goodman. *Statistical Optics*. Wiley Series in Pure and Applied Optics. Wiley, (2000).

[10] E.L. Saldin, E.A. Schneidmiller, and M.V. Yurkov. *Optics Communications*, 212(4), pp. 377–390, 2002. doi:10.1016/S0030-4018(02)02008-4